Final Draft
of the original manuscript:

Okulov, I.V.; Volegov, A.S.; Attar, H.; Boenisch, M.; Ehtemam-Haghighi, S.; Calin, M.; Eckert, J.:

Composition optimization of low modulus and high-strength TiNb-based alloys for biomedical applications

In: Journal of the Mechanical Behavior of Biomedical Materials (2016)
Elsevier

DOI: 10.1016/j.jmbbm.2016.10.013

Composition optimization of low modulus and high-strength TiNb-based alloys for biomedical applications

I. V. Okulov[a,b,c*], A. S. Volegov[a,d], H. Attar[e], M. Bönisch[a], S. Ehtemam-Haghighi[e], M. Calin[a] and J. Eckert[f,g]

[a]IFW Dresden, Institute for Complex Materials, Helmholtzstraße 20, D-01069 Dresden, Germany

[b]TU Dresden, Institut für Werkstoffwissenschaft, D-01062 Dresden, Germany

[c]Institute of Materials Research, Materials Mechanics, Helmholtz-Zentrum Geesthacht, Geesthacht, Germany

[d]Institute of Natural Sciences, Ural Federal University, 620000 Ekaterinburg, Russia

[e]School of Engineering, Edith Cowan University, 270 Joondalup Drive, Joondalup, Perth, WA 6027, Australia

[f]Erich Schmid Institute of Materials Science, Austrian Academy of Sciences (ÖAW), Jahnstraße 12, A-8700 Leoben, Austria

[g]Department Materials Physics, Montanuniversität Leoben, Jahnstraße 12, A-8700 Leoben, Austria

Abstract

The effect of chemical composition on microstructure and tensile properties of a series of low modulus Ti-Nb-Cu-Ni-Al alloys was studied. These alloys consist of primary micrometer-sized β-Ti dendrites surrounded by intermetallic phases. The morphology of the intermetallic phases is strongly affected by composition. Due to the composite microstructure, the alloys exhibit a low Young's modulus (77 – 84 GPa) together with a high yield strength of about 1000 MPa as well as moderate tensile ductility. The results demonstrate that complete substitution of Al by Ti reduces the Young's modulus by 5 %. Increasing Nb content at the expense of Ti causes a significant improvement of tensile ductility.

Keywords: titanium alloy; biomedical alloy; implant material; low Young's modulus; deformation mechanism

*Corresponding author E-mail: okulovilya@yandex.ru

Introduction

Metallic biomaterials – the materials of choice for orthopedic implants – are fundamental to improve the quality of life and longevity of human beings (Geetha et al., 2009). The commonly used metallic implant materials like stainless steel, Co-Cr or Ti-6Al-4V alloys exhibit several times higher Young's modulus values (120 – 210 GPa) compared to that of human bone (0.1 – 30 GPa) (Callister, 2007; Long and Rack, 1998; Park and Bronyino, 2000; Smallman and Bishop, 1999). A large difference in Young's modulus between a metallic implant and bone leads to a disproportionate load distribution, known as load or stress shielding effect (Geetha et al., 2009; Niinomi, 2008a). Since the health of bone is determined by the applied loads, this load shielding tends to induce a loss of bone mass (Geetha et al., 2009; Park and Bronyino, 2000). Therefore, the optimization of mechanical compatibility, in particular, lowering of the Young's modulus to mimic that of bones is a main challenge for developing of new biomedical metallic alloys for load-bearing implants. Additionally, a successful implant material for load-bearing applications should possess excellent biocompatibility, superior corrosion resistance in the body environment, and must be free of cytotoxicity (Geetha et al., 2009; Long and Rack, 1998; Tane et al., 2011).

Among metallic materials, titanium (Ti) alloys exhibit the most suitable characteristics for biomedical applications (Bönisch et al., 2015; Geetha et al., 2009; Niinomi, 2008b, 1998; Niinomi et al., 2012) what particularly has led to an increasing interest in the development of new Ti-based materials over the past years (Attar et al., 2015; H. Attar et al., 2014; Hooyar Attar et al., 2014; Laheurte et al., 2010; Niinomi, 2008b). Importantly, the Young's modulus of titanium alloys is the lowest among the common metallic biomaterials. Classification of titanium alloys implies, generally, three main groups, i.e. α-, (α + β)-, and β-type alloys (Ilyin et al., 2009), where the Young's modulus of the β-type titanium alloys is the lowest with values ranging from 40 to 80 GPa (Geetha et al., 2009; Long and Rack, 1998; Niinomi, 1998). In particular, the lowest Young's moduli of β-type titanium alloys are achieved in the solutionized condition (Niinomi et al., 2012). Unfortunately, the strength of solutionized titanium alloys is relatively low; for example, the yield strength of Ti–35.3Nb–5.1Ta–7.1Zr (also known as TNZT) is below 400 MPa (Niinomi et al., 2012). Therefore, an improvement of the strength characteristics of β-type titanium alloys is required for use in biomedical applications. The strengthening of β-type titanium alloys is achieved by a conventional aging treatment. This, however, leads to larger Young's modulus values (although, controlling the aging treatment allows the Young's modulus to be kept below 80 GPa) (Niinomi et al., 2012). Severe plastic deformation, such as severe cold rolling or severe cold swaging (Eschke et al., 2014; Marr et al., 2013, 2011; Romberg et al., 2013; Skrotzki et al., 2014), is highly effective in increasing the strength of titanium alloys while maintaining a low Young's modulus. The problem with this approach is that the high strength of severely deformed metals is achieved by compromising ductility (Koch, 2003, 2007; Ovid'ko, 2007).

He *et al.* reported a strategy to employ the high strength and low Young's modulus of nanomaterials for biomedical applications by creating an as-cast bimodal microstructure consisting of nanostructured intermetallic phases and coarse ductile β-Ti crystals (He and Hagiwara, 2006, 2005; He et al., 2003; I.V. Okulov et al., 2014b; I V. Okulov et al., 2014). The implant application of these alloys is problematic due to harmful alloying elements, for example, copper (Cu), nickel (Ni) and aluminum (Al) in the Ti-Nb-Cu-Ni-Al alloys (Okulov et al., 2013). Although, some toxic alloying elements, like Ni and Cu, can be tolerated by a human body in minute amounts (Burghardt et al., 2015; Park and Bronyino, 2000), Al is associated with long-term health problems (e.g. Alzheimer's disease, neuropathy and osteomalacia) and its content should be minimized (Geetha et al., 2009). In our previous investigation, we reported on the effect of lower Cu and Ni contents on microstructure and mechanical properties of a series of Ti-Nb-Cu-Ni-Al alloys (Okulov et al., 2013). These alloys are particularly interesting for future possible applications due to their high bioperformance values (ratio of yield strength-to-Young's modulus) (Matsumoto et al., 2007; Okulov et al., 2013). Here, we show the effect of reducing the amount of Al and optimizing the niobium (Nb) content on the microstructure and mechanical properties of Ti-Nb-Cu-Ni-Al alloys for biomedical applications. Since understanding the deformation mechanism is vital in order to fully exploit the mechanical performance with respect to possible application, a detailed microstructural analysis of deformed samples was carried out.

Materials and methods

The master alloys were fabricated from pure elements (99.9 wt.%) under argon atmosphere. Rod samples (diameter – 12 mm and length – 100 mm) were prepared by the inductive melting and casting into a water-cooled Cu crucible. The detailed experimental procedure of sample preparation was described elsewhere (I.V. Okulov et al., 2015, 2014a). X-ray diffractometry (XRD) (STOE STADIP) with Cu-Kα_1 radiation together with the X'Pert High Score Plus software was used for structural investigation of samples. The microstructure before and after tensile deformation was investigated by scanning electron microscopy (SEM) (Zeiss Leo Gemini 1530) coupled with energy-dispersive X-ray analysis (EDX) (Bruker Xflash 4010). For SEM observation, samples were mounted with conductive Cu-based resin and ground with SiC paper in the sequence 600, 1200, 2500 and 4000 grit with a Struers Rotopol machine. Finally, specimens were polished around 5 min with a solution of colloidal SiO_2 and 10 vol.% of H_2O_2 (OP-S, particle size 0.04 µm) and cleaned in the ultrasound bath for 5 min. The ImageJ image software was used to analyze size and volume fraction of phases. Flat tensile test samples with 8 mm gauge length and 1 mm thickness were tested at room temperature using an Instron 8562 testing machine at an initial strain rate of 10^{-4} s^{-1}. The strain was measured by a laser extensometer (Fiedler Optoelektronik).

Results and discussions

Microstructure

Fig. 1 shows the XRD diffractograms of the developed alloys in the as-cast state. According to XRD analysis, the alloys are β-type alloys (space group of the β-Ti phase: *Im-3m*) with some amount of intermetallic Ti_2Cu phase (space group: *I4/mmm*). These phases were also reported for the precursor $Ti_{68.8}Nb_{13.6}Cu_6Ni_{5.1}Al_{6.5}$ alloy (Okulov et al., 2013). The $Ti_{65.8}Nb_{16.6}Cu_6Ni_{5.1}Al_{6.5}$ alloy contains additionally a minor fraction of the intermetallic TiNi phase (space group: *Pm-3m*). The lattice parameter of this TiNi is a_0 = 0.3051 ± 0.0001 nm.

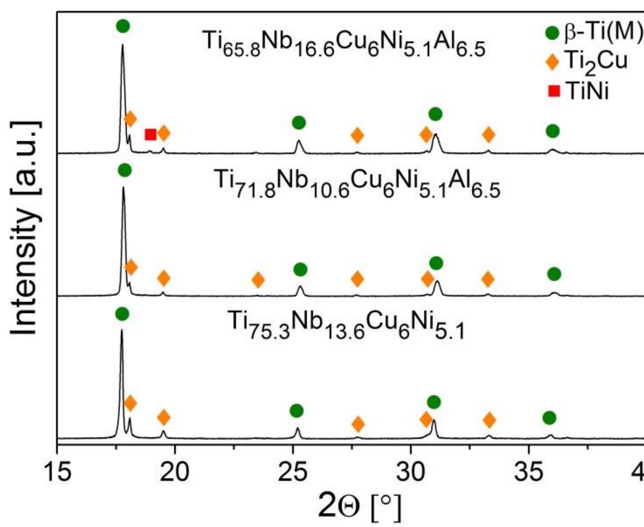

Fig. 1 *XRD patterns of the alloys developed in this study in the as-cast state*

The lattice parameter of the β-Ti phase increases from $Ti_{71.8}Nb_{10.6}Cu_6Ni_{5.1}Al_{6.5}$ (a_0 = 0.3239 ± 0.0001 nm) to $Ti_{65.8}Nb_{16.6}Cu_6Ni_{5.1}Al_{6.5}$ (a_0 = 0.3247 ± 0.0001 nm) due to the increasing amount of Nb forming a solid solution with Ti (I.V. Okulov et al., 2015; Okulov et al., 2013). The further increase of the β-Ti phase lattice parameter in $Ti_{75.3}Nb_{13.6}Cu_6Ni_{5.1}$

(a_0 = 0.3253 ± 0.0001 nm) is, most likely, due to the removal of Al, which possesses a lower atomic radius compared with Ti.

Fig. 2 presents the microstructure of the studied alloys in the as-cast state. The β-Ti phase exhibits dendritic morphology. The intermetallic phases, i.e. Ti_2Cu and TiNi, are distributed between the β-Ti dendrites. The volume fraction of the β-Ti phase is 90 ± 2 vol. % for all three compositions. These values are very close to that of 86 ± 2 vol. % of the precursor $Ti_{68.8}Nb_{13.6}Cu_6Ni_{5.1}Al_{6.5}$ alloy (Okulov et al., 2013). Thus, increasing or decreasing the Nb content by 3 at% at the cost of Ti relative to the precursor alloy as well as complete substitution of Al by Ti do not lead to notable changes of the volume fraction of the β-Ti phase.

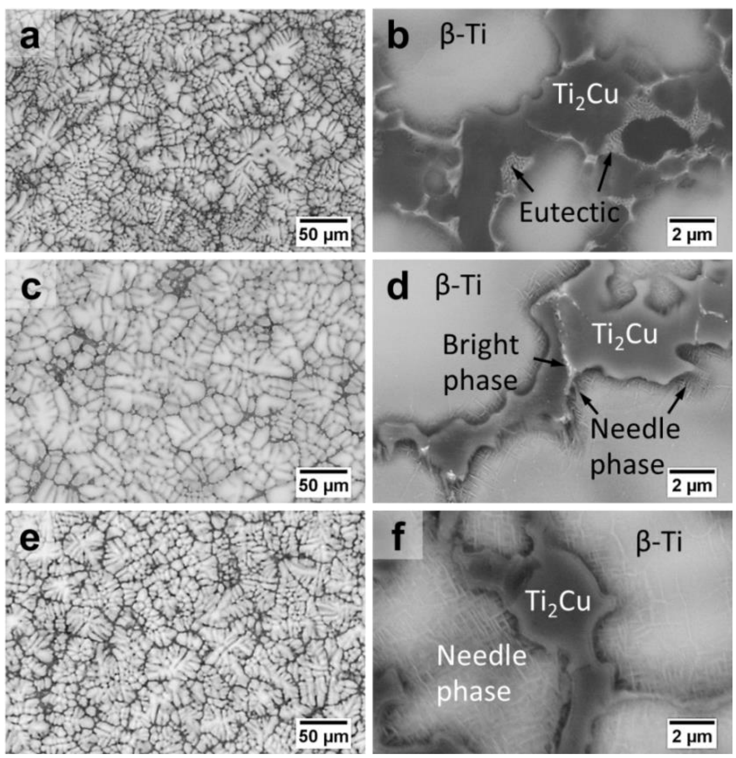

Fig. 2 *SEM backscattered electron images (BSE) of the studied alloys in the as-cast state. (a) and (b)* $Ti_{65.8}Nb_{16.6}Cu_6Ni_{5.1}Al_{6.5}$*; (c) and (d)* $Ti_{71.8}Nb_{10.6}Cu_6Ni_{5.1}Al_{6.5}$*; (e) and (f)* $Ti_{75.3}Nb_{13.6}Cu_6Ni_{5.1}$

A more detailed analysis of the microstructure (Figs. 2 d and f) shows that the periphery of the β-Ti dendrites is decorated by an unknown nanoscale needle-shaped phase in $Ti_{71.8}Nb_{10.6}Cu_6Ni_{5.1}Al_{6.5}$ and the Al-free alloy. A similar needle-shaped phase was reported in (Helth et al., 2013). Helth *et al.* have found that this phase is enriched in Cu and Ni and depleted in Nb and Al. Due to immiscibility of Cu and Nb as well as the miscibility of Ni and Cu, both Cu and Ni segregate from the Nb-rich dendrites to their periphery and, probably, stimulate the formation of the needle-shaped phase.

The microstructure of the intermetallic phases surrounding the dendrites is affected by the chemical composition of the alloys. For example, the interdendritic constituents of $Ti_{65.8}Nb_{16.6}Cu_6Ni_{5.1}Al_{6.5}$ consist of micrometer-sized Ti_2Cu grains and an ultrafine-grained eutectic (Figs. 2 a and b) while in case of $Ti_{75.3}Nb_{13.6}Cu_6Ni_{5.1}$ the interdendritic regions contain only micrometer-sized Ti_2Cu grains (Figs. 2 e and f). The $Ti_{71.8}Nb_{10.6}Cu_6Ni_{5.1}Al_{6.5}$ alloy occupies an intermediate position; its interdendritic regions are also composed of micrometer-sized Ti_2Cu decorated by a minor amount of an unknown bright phase (Figs. 2 c and d). This bright phase was not detected by XRD probably due to its low volume fraction. Since the backscattered electron contrast reflects the mean atomic number, the bright phase exhibits a higher mean atomic number compared to the Ti_2Cu phase. Therefore, we assume that this bright phase is an intermetallic TiNi phase. Thus, the optimization of intermetallic phases can be controlled by carefully adjusting the Nb and Al contents in the Ti-Nb-Cu-Ni-Al alloys. In particular, decreasing Nb or/and Al contents leads to a disappearance of the TiNi phase and, consequently, to vanishing of the ultrafine eutectic.

Mechanical properties

Typical tensile true stress-strain curves of the studied alloys are shown in Fig. 3 a. The alloys exhibit a high yield strength (1000 – 1050 MPa) together with a low Young's modulus (77 – 84 GPa) already in their as-cast state (Fig. 3 a, inset). It has to be noted that the Young's modulus of the alloys notably reduces from 84 GPa to 77 GPa as Al and Nb contents lessen. The reduction of Al and Nb causes the microstructural changes and alteration in the chemical composition of phases; in particular, it leads to formation of the bright needle phase and vanishing the TiNi phase in $Ti_{75.3}Nb_{13.6}Cu_6Ni_{5.1}$. The microstructural changes promote reduction of Young's modulus. Due to the strain-hardening behavior observed upon tensile deformation, the ultimate strength of the alloys reaches over 1100 MPa (Fig. 3 a). These strength characteristics make the studied alloys comparable with some Ti-based (Ha et al., 2012a, 2012b) and Zr-based metallic glass composites (I. V. Okulov et al., 2015).

The ductility of the alloys with lower Nb content, i.e. $Ti_{75.3}Nb_{13.6}Cu_6Ni_{5.1}$ and $Ti_{71.8}Nb_{10.6}Cu_6Ni_{5.1}Al_{6.5}$, is less than half the ductility of $Ti_{65.8}Nb_{16.6}Cu_6Ni_{5.1}Al_{6.5}$ (Fig. 3 a). This may be related to the needle-shaped phase, whose volume fraction increases at lower Nb and Al concentrations. The effect of the microstructure on the tensile ductility has been investigated by detailed microstructural examination of deformed samples, as will be presented below.

Fig. 3 b presents strength and Young's modulus data for commercials biomedical titanium alloys. The contours show the mechanical bioperformance (ratio of yield strength-to-Young's modulus) of the materials: the higher the value is the more the material is suitable for implant applications (Geetha et al., 2009; Guo et al., 2012). The bioperformance values of the developed alloys are among the largest values for bioapplicable titanium alloys. Thus, the developed alloys for this study exhibit a potential for application as load-bearing implant materials.

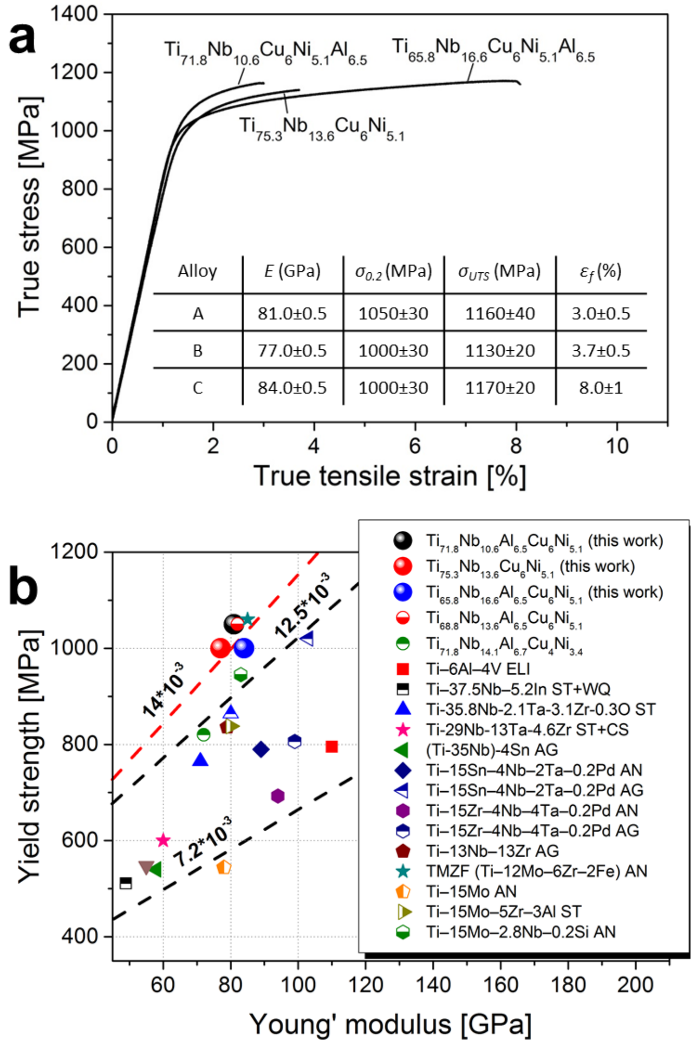

Alloy	E (GPa)	$\sigma_{0.2}$ (MPa)	σ_{UTS} (MPa)	ε_f (%)
A	81.0±0.5	1050±30	1160±40	3.0±0.5
B	77.0±0.5	1000±30	1130±20	3.7±0.5
C	84.0±0.5	1000±30	1170±20	8.0±1

Fig. 3 *(a) True stress-true strain curves under tensile loading at room temperature (Note: "A" denotes $Ti_{71.8}Nb_{10.6}Cu_6Ni_{5.1}Al_{6.5}$, "B" - $Ti_{75.3}Nb_{13.6}Cu_6Ni_{5.1}$, "C" - $Ti_{65.8}Nb_{16.6}Cu_6Ni_{5.1}Al_{6.5}$, E – Young's modulus, $\sigma_{0.2}$ – yield strength, σ_{UTS} – ultimate strength and ε_f – strain at fracture). (b) Yield strength plotted against Young's modulus for commercial biomedical titanium alloys and*

the studied alloys of this work (Note: AN – annealed, AG – aged, ST – solution treated, WQ– water quenched, CS – cold swaged); the dashed contours show the bioperformance $\sigma_{0.2}/E$. The data are from (Calin et al., 2014; Furuta et al., 2005; Matsumoto et al., 2005; Niinomi, 1998; Niinomi et al., 2002; Okulov et al., 2013).

Deformation mechanism

Fig. 4 presents the typical microstructure of samples deformed until fracture. The SEM micrographs reveal plastic deformation of the β-Ti dendrites by slip (Figs. 4 a, c, and e). Additionally, the intermetallic Ti_2Cu phase shows some plastic deformation, what is, particularly, depicted in the inset of Fig. 4 a.

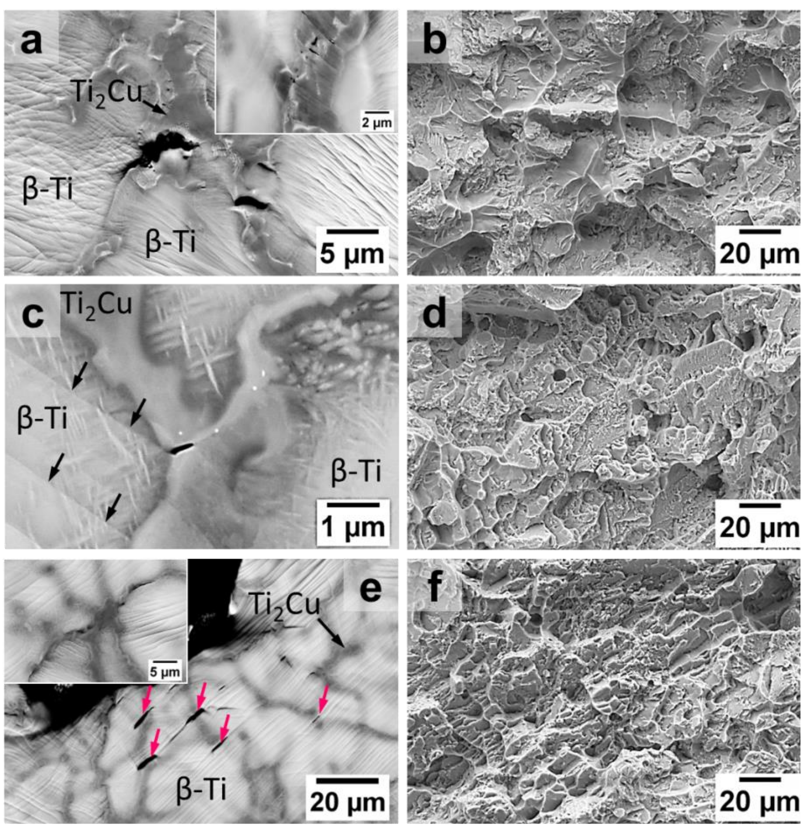

Fig. 4 *SEM micrographs of the developed alloys deformed to fracture. Surface microstructure (a) and fracture surface (b) of* $Ti_{65.8}Nb_{16.6}Cu_6Ni_{5.1}Al_{6.5}$*. Surface microstructure (c) and fracture surface (d) of* $Ti_{71.8}Nb_{10.6}Cu_6Ni_{5.1}Al_{6.5}$ *(Note: arrows indicate blocked slip bands). Surface microstructure (e) and fracture surface (f) of* $Ti_{75.3}Nb_{13.6}Cu_6Ni_{5.1}$ *(Note: unlabeled arrows indicate cracks in the interior of* Ti_2Cu*)*

There is also evidence that some slip bands formed in the dendrites penetrate the Ti_2Cu grains similar to what was found for the precursor alloy (Okulov et al., 2013). This causes formation of cracks along these slip bands which then propagate into the interior of the Ti_2Cu phase as shown in Figs. 4 a and e. However, some slip bands formed in the dendrites are blocked at the interface between β-Ti and Ti_2Cu phases (Figs. 4 c). It was found that some of these blocked slip events promote crack formation in the Ti_2Cu phase (Figs. 4 c). Generally, cracks in the interior of the Ti_2Cu phase are observed for all alloys investigated in this study. The cracks are arrested by the β-Ti dendrites indicating their good toughness, similar as it has also been reported previously for Ti-Nb-Ni-Co-Al alloys (I.V. Okulov et al., 2014c). Interestingly, there are no evidences of crack formation along the needle-shaped particles. The penetration of the needle-shaped particles by slip bands indicates a coherent/semi-coherent relationship of this phase with β-Ti (Fig. 4 c).

The fracture surface of the most ductile $Ti_{65.8}Nb_{16.6}Cu_6Ni_{5.1}Al_{6.5}$ alloy exhibits dimple features mixed with quasi-cleavage fracture (Fig. 4 b). This large dimple features correspond to the size of the dendrites and, therefore, formed due to rapture of these ductile dendrites. The quasi-cleavage features likely form upon rapture of interdendritic regions containing intermetallic

Ti_2Cu particles. The alloys with lower Nb content, i.e. $Ti_{75.3}Nb_{13.6}Cu_6Ni_{5.1}$ and $Ti_{71.8}Nb_{10.6}Cu_6Ni_{5.1}Al_{6.5}$, exhibit quasi-cleavage fracture (Figs. 4 d and f) independently on the Al content. In a view of similar volume fraction of intermetallic phases, it seems that the decreasing Nb content from 16.6 at% to 13.6 at% is critical for the ductility of the dendritic phase leading to a lowering of the ductility of these alloys.

From these findings one can conclude that the slip bands formed in the β-Ti dendrites exhibit different types of interactions with the grain boundaries, in particular: (i) penetration of slip bands into the Ti_2Cu phase, (ii) blocking of slip bands at the β-Ti/Ti_2Cu interface leading to crack formation, and (iii) blocking of slip bands at the β-Ti/Ti_2Cu interface without crack formation. The most critical factor for slip penetration is the alignment of slip systems of neighboring grains (Guo et al., 2014; I.V. Okulov et al., 2014a). In particular, slip penetration was observed for the cube-on-cube oriented crystals in the $Ti_{68.8}Nb_{13.6}Co_6Cu_{5.1}Al_{6.5}$ alloy (I.V. Okulov et al., 2014a). In the current case, the slip penetration occurred from the bcc β-Ti into the Ti_2Cu phase, which is not a cubic structure but tetragonal. This suggests that the slip systems of some neighboring bcc β-Ti and Ti_2Cu crystals are aligned to each other. The blocking of slips is probably due to less favorable oriented slip systems in the neighboring crystals with the incoming slip system (Guo et al., 2014; I.V. Okulov et al., 2014a).

The plastic deformation of the alloys leads to the formation of slip bands in the interior of the β-Ti dendrites and, under certain conditions, these slip bands penetrate Ti_2Cu grains causing crack formation in their interior. These cracks are arrested by the dendrites causing them to grow and transforms into voids at increasing strain. Obviously, the ability of the β-Ti dendrites, as primary phase, to arrest the crack propagation at higher strains determines the plasticity of the alloys. The difference in chemical composition of the alloys affects the mechanical properties of the β-Ti dendrites and, in particular, an increasing Nb concentration favors larger plastic deformation. Yet, other factors like interconnectivity of the intermetallic network related to the interdendritic crack propagation are import for the tensile ductility of this type of alloys (I.V. Okulov et al., 2014c; I V. Okulov et al., 2014). However, both fracture surface morphology and absence of continuous cracks passing through the intermetallic network are indicative against such a failure scenario.

Conclusions

The chemical composition of Ti-Nb-Cu-Ni-Al alloys was optimized to reduce the amount of harmful elements and improve the mechanical performance. Along this line, $Ti_{65.8}Nb_{16.6}Cu_6Ni_{5.1}Al_{6.5}$, $Ti_{71.8}Nb_{10.6}Cu_6Ni_{5.1}Al_{6.5}$ and $Ti_{75.3}Nb_{13.6}Cu_6Ni_{5.1}$ alloys were developed. The microstructure of the alloys consists of β-Ti dendrites and about 10 vol% of intermetallic phases (mainly Ti_2Cu) surrounding the dendrites. Due to the composite microstructure, the alloys exhibit high yield strength (1000 – 1050 MPa) along with low Young's modulus (77 – 84 GPa). Complete substitution of harmful Al by Ti leads to improvement of the biomechanical performance, in particular, to lowering the Young's modulus by 5 %. The increase of the Nb content at the expense of Ti causes a significant tensile ductility improvement from 3 to 8 % strain. The plastic deformation of the alloys begins with the deformation of the softer β-Ti dendrites by slip. The slip bands formed in the β-Ti dendrites exhibit different types of interactions with the β-Ti/Ti_2Cu interface, in particular: (i) penetration of slip bands into the

Ti_2Cu phase, (ii) blocking of slip bands at the β-Ti/Ti_2Cu interface leading to crack formation, and (iii) blocking of slip bands at the β-Ti/Ti_2Cu interface without crack formation. The cracks formed into the interior of intermetallics are getting arrested by the β-Ti dendrites. This causes growth and transformation of cracks into voids at increasing strains, consequently, promoting rupture.

Acknowledgments

The authors thank S. Donath, F. Ebert and M. Frey for technical support. This work benefited from financial support by the European Commission within the framework of the FP7-MCITN Network BioTiNet (PITN-GA-2010-264635), the EU and the Free State of Saxony (contract number 100111842) within the European Centre for Emerging Materials and Processes Dresden (ECEMP) and Act 211 Government of the Russian Federation (contract number 02.A03.21.0006). Additional support through the German Science Foundation (DFG) under the Leibniz Program (grant EC 111/26-1) and the European Research Council under the ERC Advanced Grant INTELHYB (grant ERC-2013-ADG-340025) is gratefully acknowledged.

References

Attar, H., Bönisch, M., Calin, M., Zhang, L.C., Scudino, S., Eckert, J., 2014. Selective laser melting of in situ titanium-titanium boride composites: Processing, microstructure and mechanical properties. Acta Mater. 76, 13–22. doi:10.1016/j.actamat.2014.05.022

Attar, H., Calin, M., Zhang, L.C., Scudino, S., Eckert, J., 2014. Manufacture by selective laser melting and mechanical behavior of commercially pure titanium. Mater. Sci. Eng. A 593, 170–177. doi:10.1016/j.msea.2013.11.038

Attar, H., Prashanth, K.G., Zhang, L.-C., Calin, M., Okulov, I. V., Scudino, S., Yang, C., Eckert, J., 2015. Effect of Powder Particle Shape on the Properties of In Situ Ti–TiB Composite Materials Produced by Selective Laser Melting. J. Mater. Sci. Technol. 31, 1001–1005. doi:10.1016/j.jmst.2015.08.007

Bönisch, M., Calin, M., Van Humbeeck, J., Skrotzki, W., Eckert, J., 2015. Factors influencing the elastic moduli, reversible strains and hysteresis loops in martensitic Ti-Nb alloys. Mater. Sci. Eng. C 48, 511–520. doi:10.1016/j.msec.2014.12.048

Burghardt, I., Lüthen, F., Prinz, C., Kreikemeyer, B., Zietz, C., Neumann, H.G., Rychly, J., 2015. A dual function of copper in designing regenerative implants. Biomaterials 44, 36–44. doi:10.1016/j.biomaterials.2014.12.022

Calin, M., Helth, A., Gutierrez Moreno, J.J., Bönisch, M., Brackmann, V., Giebeler, L., Gemming, T., Lekka, C.E., Gebert, A., Schnettler, R., Eckert, J., 2014. Elastic softening of β-type Ti-Nb alloys by indium (In) additions. J. Mech. Behav. Biomed. Mater. 39, 162–174.

doi:10.1016/j.jmbbm.2014.07.010

Callister, W.D., 2007. Materials Science and Engineering: An Introduction. John Wiley & Sons, Inc., New York.

Eschke, A., Scharnweber, J., Oertel, C.-G., Skrotzki, W., Marr, T., Romberg, J., Freudenberger, J., Schultz, L., Okulov, I., Kühn, U., Eckert, J., 2014. Texture development in Ti/Al filament wires produced by accumulative swaging and bundling. Mater. Sci. Eng. A 607, 360–367. doi:10.1016/j.msea.2014.04.003

Furuta, T., Kuramoto, S., Hwang, J., Nishino, K., Saito, T., 2005. Elastic deformation behavior of multi-functional Ti-Nb-Ta-Zr-O alloys. Mater. Trans. 46, 3001–3007. doi:10.2320/matertrans.46.3001

Geetha, M., Singh, A.K., Asokamani, R., Gogia, A.K., 2009. Ti based biomaterials, the ultimate choice for orthopaedic implants – A review. Prog. Mater. Sci. 54, 397–425. doi:10.1016/j.pmatsci.2008.06.004

Guo, S., Bao, Z., Meng, Q., Hu, L., Zhao, X., 2012. A Novel Metastable Ti-25Nb-2Mo-4Sn Alloy with High Strength and Low Young's Modulus. Metall. Mater. Trans. A 43, 3447–3451. doi:10.1007/s11661-012-1324-0

Guo, Y., Britton, T.B., Wilkinson, A.J., 2014. Slip band–grain boundary interactions in commercial-purity titanium. Acta Mater. 76, 1–12. doi:10.1016/j.actamat.2014.05.015

Ha, D.J., Kim, C.P., Lee, S., 2012a. Correlation of microstructure and tensile properties of Ti-based amorphous matrix composites modified from conventional titanium alloys. Mater.

Sci. Eng. A 558, 558–565. doi:10.1016/j.msea.2012.08.048

Ha, D.J., Kim, C.P., Lee, S., 2012b. Tensile deformation behavior of two Ti-based amorphous matrix composites containing ductile β dendrites. Mater. Sci. Eng. A 552, 404–409. doi:10.1016/j.msea.2012.05.061

He, G., Eckert, J., Dai, Q.L., Sui, M.L., Löser, W., Hagiwara, M., Ma, E., 2003. Nanostructured Ti-based multi-component alloys with potential for biomedical applications. Biomaterials 24, 5115–5120. doi:10.1016/S0142-9612(03)00440-X

He, G., Hagiwara, M., 2006. Ti alloy design strategy for biomedical applications. Mater. Sci. Eng. C 26, 14–19. doi:10.1016/j.msec.2005.03.007

He, G., Hagiwara, M., 2005. Bimodal structured Ti-base alloy with large elasticity and low Young's modulus. Mater. Sci. Eng. C 25, 290–295. doi:10.1016/j.msec.2005.03.001

Helth, A., Siegel, U., Kühn, U., Gemming, T., Gruner, W., Oswald, S., Marr, T., Freudenberger, J., Scharnweber, J., Oertel, C.-G., Skrotzki, W., Schultz, L., Eckert, J., 2013. Influence of boron and oxygen on the microstructure and mechanical properties of high-strength Ti66Nb13Cu8Ni6.8Al6.2 alloys. Acta Mater. 61, 3324–3334. doi:10.1016/j.actamat.2013.02.022

Ilyin, A.A., Kolachev, B.A., Polkin, I.S., 2009. Titanium Alloys. Composition, Structure, Properties. Reference book. VILS-MATI, Moscow.

Koch, C., 2003. Optimization of strength and ductility in nanocrystalline and ultrafine grained metals. Scr. Mater. 49, 657–662. doi:10.1016/S1359-6462(03)00394-4

Koch, C.C., 2007. Structural nanocrystalline materials: an overview. J. Mater. Sci. 42, 1403–1414. doi:10.1007/s10853-006-0609-3

Laheurte, P., Prima, F., Eberhardt, A., Gloriant, T., Wary, M., Patoor, E., 2010. Mechanical properties of low modulus beta titanium alloys designed from the electronic approach. J. Mech. Behav. Biomed. Mater. 3, 565–573. doi:10.1016/j.jmbbm.2010.07.001

Long, M., Rack, H.J., 1998. Titanium alloys in total joint replacement--a materials science perspective. Biomaterials 19, 1621–1639. doi:10.1016/S0142-9612(97)00146-4

Marr, T., Freudenberger, J., Kauffmann, A., Romberg, J., Okulov, I., Petters, R., Scharnweber, J., Eschke, A., Oertel, C.-G., Kühn, U., Eckert, J., Skrotzki, W., Schultz, L., 2013. Processing of Intermetallic Titanium Aluminide Wires. Metals (Basel). 3, 188–201. doi:10.3390/met3020188

Marr, T., Freudenberger, J., Seifert, D., Klauß, H., Romberg, J., Okulov, I., Scharnweber, J., Eschke, A., Oertel, C.-G., Skrotzki, W., Kühn, U., Eckert, J., Schultz, L., 2011. Ti-Al Composite Wires with High Specific Strength. Metals (Basel). 1, 79–97. doi:10.3390/met1010079

Matsumoto, H., Watanabe, S., Hanada, S., 2007. Microstructures and mechanical properties of metastable β TiNbSn alloys cold rolled and heat treated. J. Alloys Compd. 439, 146–155. doi:10.1016/j.jallcom.2006.08.267

Matsumoto, H., Watanabe, S., Hanada, S., 2005. Beta TiNbSn Alloys with Low Young's Modulus and High Strength. Mater. Trans. 46, 1070–1078. doi:10.2320/matertrans.46.1070

Niinomi, M., 2008a. Mechanical biocompatibilities of titanium alloys for biomedical applications. J. Mech. Behav. Biomed. Mater. 1, 30–42. doi:10.1016/j.jmbbm.2007.07.001

Niinomi, M., 2008b. Biologically and Mechanically Biocompatible Titanium Alloys. Mater. Trans. 49, 2170–2178. doi:10.2320/matertrans.L-MRA2008828

Niinomi, M., 1998. Mechanical properties of biomedical titanium alloys. Mater. Sci. Eng. A 243, 231–236. doi:10.1016/S0921-5093(97)00806-X

Niinomi, M., Hattori, T., Morikawa, K., Kasuga, T., Suzuki, A., Fukui, H., Niwa, S., 2002. Development of Low Rigidity Beta-type Titanium Alloy for Biomedical Applications. Mater. Trans. 43, 2970–2977. doi:10.2320/matertrans.43.2970

Niinomi, M., Nakai, M., Hieda, J., 2012. Development of new metallic alloys for biomedical applications. Acta Biomater. 8, 3888–903. doi:10.1016/j.actbio.2012.06.037

Okulov, I.V., Bönisch, M., Kühn, U., Skrotzki, W., Eckert, J., 2014a. Significant tensile ductility and toughness in an ultrafine-structured Ti68.8Nb13.6Co6Cu5.1Al6.5 bi-modal alloy. Mater. Sci. Eng. A 615, 457–463. doi:10.1016/j.msea.2014.07.108

Okulov, I.V., Kühn, U., Marr, T., Freudenberger, J., Soldatov, I.V., Schultz, L., Oertel, C.-G., Skrotzki, W., Eckert, J., 2014b. Microstructure and mechanical properties of new composite structured Ti-V-Al-Cu-Ni alloys for spring applications. Mater. Sci. Eng. A 603, 76–83. doi:10.1016/j.msea.2014.02.070

Okulov, I.V., Kühn, U., Romberg, J., Soldatov, I.V., Freudenberger, J., Schultz, L., Eschke, A., Oertel, C.-G., Skrotzki, W., Eckert, J., 2014c. Mechanical behavior and tensile/compressive strength asymmetry of ultrafine structured Ti-Nb-Ni-Co-Al alloys with bi-modal grain size distribution. Mater. Des. 62, 14–20. doi:10.1016/j.matdes.2014.05.007

Okulov, I.V., Pauly, S., Kühn, U., Gargarella, P., Marr, T., Freudenberger, J., Schultz, L., Scharnweber, J., Oertel, C.-G., Skrotzki, W., Eckert, J., 2013. Effect of microstructure on the mechanical properties of as-cast Ti–Nb–Al–Cu–Ni alloys for biomedical application. Mater. Sci. Eng. C 33, 4795–4801. doi:10.1016/j.msec.2013.07.042

Okulov, I.V., Wendrock, H., Volegov, A.S., Attar, H., Kühn, U., Skrotzki, W., Eckert, J., 2015. High strength beta titanium alloys: New design approach. Mater. Sci. Eng. A 628, 297–302. doi:10.1016/j.msea.2015.01.073

Okulov, I. V., Kühn, U., Marr, T., Freudenberger, J., Schultz, L., Oertel, C.-G., Skrotzki, W., Eckert, J., 2014. Deformation and fracture behavior of composite structured Ti-Nb-Al-Co(-Ni) alloys. Appl. Phys. Lett. 104. doi:http://dx.doi.org/10.1063/1.4865930

Okulov, I. V., Soldatov, I. V., Sarmanova, M.F., Kaban, I., Gemming, T., Edström, K., Eckert, J., 2015. Flash Joule heating for ductilization of metallic glasses. Nat. Commun. 6, 7932. doi:10.1038/ncomms8932

Ovid’ko, I.A., 2007. Review on the fracture processes in nanocrystalline materials. J. Mater. Sci. 42, 1694–1708. doi:10.1007/s10853-006-0968-9

Park, J.B., Bronyino, J.D., 2000. Biomaterials: principles and applications, 2nd ed. CRC Press, Boca Raton.

Romberg, J., Freudenberger, J., Scharnweber, J., Gaitzsch, U., Marr, T., Eschke, A., Kühn, U., Oertel, C.-G., Okulov, I., Petters, R., Skrotzki, W., Eckert, J., Schultz, L., 2013.

Metallographic Preparation of Aluminium-Titanium Composites. Pract. Metallogr. 50, 739–753. doi:10.3139/147.110259

Skrotzki, W., Eschke, A., Romberg, J., Scharnweber, J., Marr, T., Petters, R., Okulov, I., Oertel, C.-G., Freudenberger, J., Kühn, U., Schultz, L., Eckert, J., 2014. Processing of High Strength Light-Weight Metallic Composites. Adv. Eng. Mater. n/a–n/a. doi:10.1002/adem.201400190

Smallman, R.E., Bishop, R.J., 1999. Chapter 13 - Biomaterials, in: Smallman, R.E., BiShop, R.J. (Eds.), Modern Physical Metallurgy and Materials Engineering (Sixth Edition). Butterworth-Heinemann, Oxford, pp. 394–405. doi:http://dx.doi.org/10.1016/B978-075064564-5/50013-6

Tane, M., Nakano, T., Kuramoto, S., Hara, M., Niinomi, M., Takesue, N., Yano, T., Nakajima, H., 2011. Low Young’s modulus in Ti–Nb–Ta–Zr–O alloys: Cold working and oxygen effects. Acta Mater. 59, 6975–6988. doi:10.1016/j.actamat.2011.07.050